

Current direction induced rectification effect on (integer) quantized Hall plateaus

A. Siddiki

Physics Department, Arnold Sommerfeld Center for Theoretical Physics, and Center for NanoScience, Ludwig-Maximilians-Universität, Theresienstrasse 37, 80333 Munich, Germany

Current polarization induced rectification of the quantized Hall plateaus (QHPs) is studied within a Hartree type mean field approximation for asymmetrically depleted samples. We first investigate the existence of the current carrying incompressible strips (ISs), by solving the self-consistent equations, and their influence on magneto-transport (MT) properties. Next, the widths of the ISs are examined in terms of the steepness of the confining potential profile considering gate defined Hall bars. The corresponding MT coefficients are calculated using a local Ohm's law for a large fixed current and are compared for symmetric and asymmetric depleted samples. We predict that, the extend of the QHPs strongly depend on the current polarization, in the out of linear response regime, when considering asymmetrically depleted samples. Our results, concerning the extend of the QHPs depending on the current polarization are in contrast to the ones of the conventional theories of the integer quantized Hall effect (IQHE). We propose certain experimental conditions to test our theoretical predictions at high mobility, narrow samples.

PACS numbers: 73.20.-r, 73.50.Jt, 71.70.Di

Surprisingly, open questions remain even nowadays in the theory of the IQHE almost three decades after its discovery [1]. When a two dimensional electron system (2DES) is subject to a strong perpendicular magnetic B field, the energy spectrum is (Landau) quantized. Due to the gapped density of states (DOS), the measured longitudinal and Hall resistances, R_L and R_H , present anomalies if the electron density (n_{el}) is an integer multiple of the quantized magnetic flux density (n_ϕ), such that $R_L = 0$ and Hall resistance becomes quantized, i.e. $R_H = \frac{e^2}{\nu h}$, where filling factor $\nu (= n_{el}/n_\phi)$ is an integer, e is the electron charge and h is Planck's constant. In a first order approximation, two main schools have emerged in giving an explanation to the IQHE, namely the bulk [2] and the edge [3, 4, 5] pictures, which are thought to be unavoidably in contrast to each other in answering the question "where does the current flow?". Moreover, there is an ongoing debate about whether transport at the edges occur in the *compressible* [3, 5] or in the *incompressible* [6, 7, 8, 9] states, which are formed as a direct consequence of Landau quantization and their widths are determined by the Coulomb interaction. The local probe experiments present a strong evidence suggesting that the current is carried by the incompressible strips [10, 11]. In particular, experiments performed at the von Klitzing's group where a scanning force microscope was used to measure the spatial distribution of the Hall potential across the 2DES as a function of the B field [10]. The observed dependence of the potential profile on ν already suggests the dominant role of the $e - e$ interactions, leading to finite widths of both compressible and incompressible strips (ISs), where the current is carried by the later. The Hall potential profiles were categorized mainly to three types: Type I, the potential varies linearly in position $1.6 < \nu < 2$, Type II non-linear spatial variation ($\nu \approx 2$) and, Type III, where the

potential strongly varies at the edges, however, is constant at bulk, $2.05 < \nu < 2.3$. The observations were explained within the self-consistent (SC) Thomas-Fermi-Poisson theory of screening [12] plus the local Ohm's law (LOL) [7], which are the bases of the present work to be discussed later. In a subsequent theoretical work [8] the effect of finite extent of the wave functions on the incompressible strips (ISs) was simulated by a spatial averaging of the local quantities over quantum mechanical length scales such as the Fermi wavelength λ or magnetic length $l (= \sqrt{\hbar/eB})$. The spatial averaging also enabled them to relax the strict local approximation considering MT and to lift the artifacts arising from the Thomas-Fermi approximation (TFA). The main outcome of this work was to show explicitly that, if there exists an IS somewhere in the sample (which is translation invariant in the current direction) the system is in the QH regime, i.e. the widths of the QHPs strongly depend on the widths of the ISs. Moreover, its predictions on the asymmetry of the QHPs with respect to the classical Hall resistance curve, depending on the mobility and sample width, are confirmed experimentally [13].

In the present work, we first present our geometry and the related electrostatic problem, which in turn determines the width of the ISs. Next, we investigate the effect of a large current on the local electron density $n_{el}(x)$ using the LOL. The DOS $D(E)$ and the MT coefficients are obtained from the SC Born approximation [14]. The current density $\mathbf{j}(\mathbf{r})$, $n_{el}(x)$ and R_H are compared in the out of linear response regime (LRR) for generic and asymmetrically depleted samples. The asymmetric distribution of the ISs with respect to the center of the sample and its effect on R_H is utilized as an experimental test for two different boundary conditions, thereby density profiles. At asymmetrically depleted samples, in which the potential profile is steeper at one side than the other,

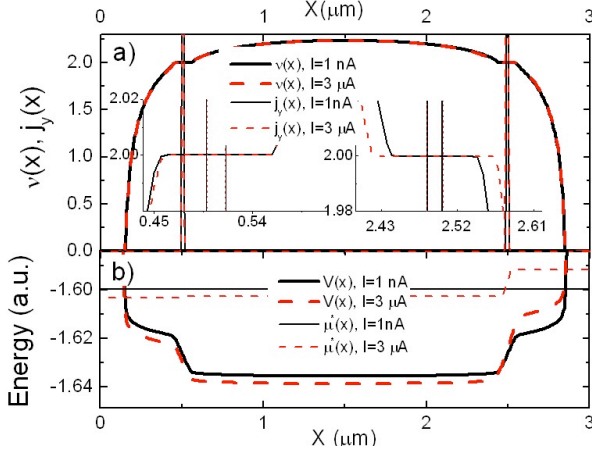


FIG. 1: (Color online) (a) The spatial distribution of $\nu(x)$ and the corresponding $j_y(x)$ considering a generic (symmetric, i.e. $b_l = b_r = 150 \text{ nm}$, assuming $V_L = V_R = 0$) $3 \mu\text{m}$ sample. (b) The SC and electrochemical potentials under low (solid lines) and high bias (broken lines). All calculations are done for $\hbar(eB/m)/E_F^0 (= \Omega/E_F^0) = 0.94$, where $E_F^0 (= 12.75 \text{ meV})$ is the Fermi energy at the center, i.e. $X = 1.5 \mu\text{m}$, at the default temperature $k_B T/\Omega = 0.025$. A homogeneous donor density of $n_0 = 4 \times 10^{11} \text{ cm}^{-2}$ is assumed, with the impurity parameter $\Gamma/\Omega = 0.03$.

we show that the IS at the steep edge is narrower than the one at the smoother edge, which in turn determines the current distribution and the extend of QHPs. As a result of the applied current a Hall potential develops within the sample, whose slope is determined by the current direction and amplitude. Therefore, if the Hall potential added to the electrostatic potential has the same slope sign with the SC potential where the narrow IS resides, this IS is enlarged and the QHP becomes wider otherwise, becomes narrower. Such a rectification effect due to current polarization is counter intuitive considering the conventional theories, both bulk and the edge, since the extend of the QHPs mainly depend on the mobility at fixed temperature and current amplitude, not its direction. Here we follow the path of Ref. [8] in de-

scribing our 2DES considering the historical Chklovskii geometry [15], i.e. a translation invariance in y - (current) direction, where donor distribution n_0 is assumed to be homogeneous residing together with the electron layer on $z = 0$ plane and the 2DES is depleted from the edges by applying V_L and V_R to the metallic gates on sides. In the screening theory of the IQHE, the Coulomb interaction is included to a spin degenerate single particle Hamiltonian, within the a Hartree type approximation, via adding an effective mean field potential given by

$$V_H(x) = \frac{2e^2}{\kappa} \int_{-d}^d n_{\text{el}}(t) K(x, t) dt, \quad (1)$$

where κ is an average dielectric constant ($= 12.4$ for GaAs) at the interface of the 2DES and the kernel $K(x, t)$ preserves the boundary conditions $V(-d) = V_L$ and $V(d) = V_R$ for the above described model. The total potential (energy) is then

$$V(x) = V_{bg}(x) + V_G(x) + V_H(x) \quad (2)$$

where $V_{bg}(x)$ is the background potential generated by the donors and $V_G(x)$ by the gates for a sample width of $2d$. To calculate the Hartree potential one needs the electron density distribution, which is given within TFA by

$$n_{\text{el}}(x) = \int dE D(E) \left[e^{\frac{E - \mu(x)}{k_B T}} + 1 \right]^{-1}, \quad (3)$$

where k_B is the Boltzmann constant, T the temperature, $\mu(x) = \mu_{\text{eq}}^* - V(x)$ the electrochemical potential and μ_{eq}^* the chemical potential at equilibrium. We define the widths Γ of the broadened Landau levels (LLs) from the mobility dependent short range broadening [8, 14]. The SC scheme is closed by the Eqns. 2 and 3 provided that the left and right depletion lengths, b_l and b_r , are given. The numerical task is now to solve these equations by iteration until the electron density distribution remains unchanged up to a numerical accuracy of 10^{-8} . In the next step the local current density $\mathbf{j}(\mathbf{r})$ is calculated assuming a fixed current in y direction $I = \int_{-d}^d j_y(x, y) dx$ via Ohm's law

$$\nabla \mu^*(\mathbf{r})/\mathbf{e} \equiv \mathbf{E}(\mathbf{r}) = \hat{\rho}(\mathbf{r})\mathbf{j}(\mathbf{r}), \quad (4)$$

provided that the resistivity tensor $\hat{\rho}(\mathbf{r})$ is known through the DOS [7, 8] and assuming a stationary state using the local electric field $\mathbf{E}(\mathbf{r})$ obtained in the previous step. The translation invariance is utilized together with the equation of continuity $\nabla \cdot \mathbf{j}(\mathbf{r}) = \mathbf{0}$ and $\nabla \times \mathbf{E}(\mathbf{r}) = \mathbf{0}$ to obtain

$$j_x \equiv 0, \quad E_y(x) \equiv E_y^0, \quad (5)$$

$$j_y(x) = E_y^0/\rho_L(x), \quad E_x(x) = E_y^0 \rho_H(x)/\rho_L(x),$$

where $\rho_L(x)$ and $\rho_H(x)$ are the diagonal and off-diagonal entries of the resistivity tensor, respectively, and the constant electric field in y direction $E_y^0 = I \cdot \left[\int_{-d}^d \frac{dx}{\rho_L(x)} \right]^{-1}$.

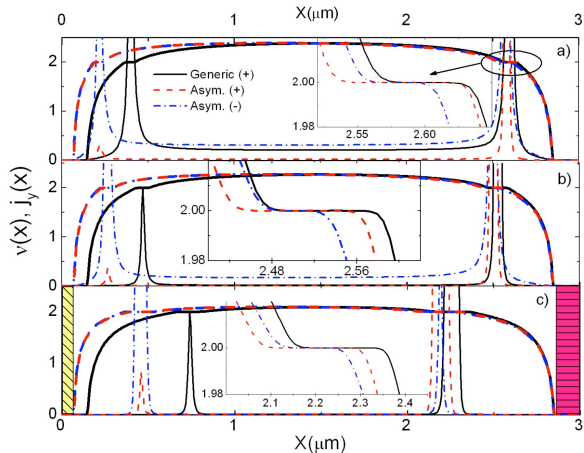


FIG. 2: (Color online) The local variation of the filling factor and the current densities for three selected B values, indicated in Fig. 3, considering: (i) generic (black solid line) and (ii) asymmetric samples, by setting $V_L = 0$ and $V_R = -1.1$ V which results in $b_l = b_r/2 = 75$ nm. Current polarizations are depicted by (red) broken lines for (+) and (blue) dash-dotted lines for (-). The asymmetric depletion is shown by the diagonal shaded region on LHS and horizontal shaded region on RHS (c), which results in $E_F^0 = 13.12$ meV. Insets show the regions of ISs on the right side.

Then $\mu^*(x)$ (now position dependent) is obtained from Eqn. 4 by integration, up to a constant which is fixed by n_{el} . In our numerical scheme we start with $n_{\text{el}}(x)$ calculated without current, then calculate the current distribution for a given fixed I . Next, we obtain $\mu^*(x)$ such that n_{el} is kept constant and start the new iteration from the newly calculated $n_{\text{el}}(x)$. This procedure is continued until convergence is obtained. In this paper we apply the above described calculation scheme to an asymmetrically depleted gate defined sample. Following Ref. [8], we perform a spatial averaging over λ (~ 33 nm) to simulate the effects of the finite extend of the wave functions, which also lifts the local strictness of the Ohm's law. We show that the large current induces an asymmetry on the widths of the ISs due to the tilting of the Landau levels

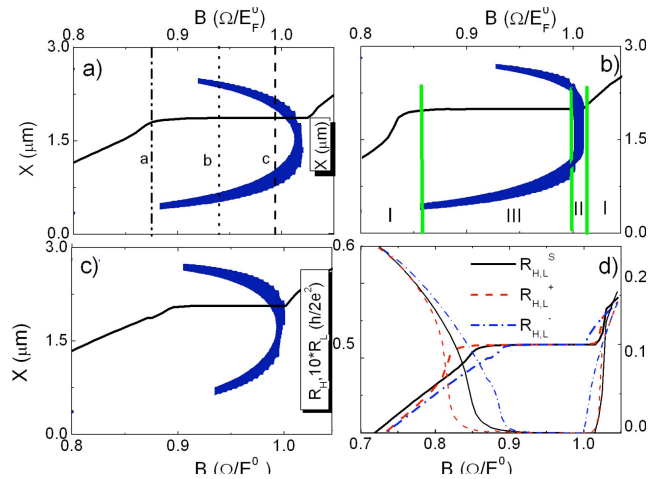


FIG. 3: (Color online) The spatial distribution of the ISs (blue regions) as a function of B for generic (a) and asymmetric samples with (+) (b) and (-) DC polarization (c). The corresponding R_H and R_L (d). Vertical lines indicate the B field values shown in Fig. 2.

as a result of self-consistency, i.e. adding the Hall potential to the total potential and recalculating the electron density. The amplitude of the current $I \sim 3 \mu\text{A}$ is sufficiently large being in the out of LRR. Our aim is, first to present this current induced asymmetry calculated for a generic sample, which is equally and largely depleted from both edges. Next using the side gates, we deplete the sample asymmetrically such that the potential on the right hand side (RHS) is smoother than that of the left hand side (LHS). Therefore, the IS on RHS is larger even without any current induced effect. In the last step we apply a large negative (-) and a positive (+) DC current to the system and investigate its effect on the density distribution and the widths of the QHPs.

The applied current introduces a Hall voltage, which is added to the SC potential, hence tilts the LLs and electrons are redistributed accordingly. As a consequence of a (+) bias, if there exists an IS, the spatial extend of the energy gapped region on the RHS becomes wider, whereas

shrinks on the LHS, resulting in a wider IS on the RHS and a narrower IS on the LHS. Such a situation is shown in Fig.1a. The local electron distributions (or equivalently the local filling factor $\nu(x) = 2\pi l^2$) calculated at low (thick solid lines) and high (thick broken lines) current biases is shown together with the current density distribution (thin vertical lines) in the upper panel for a generic sample. It is clear that, the IS on the RHS is larger than the one on the LHS under the large current bias (cf. the inset of Fig. 1 and the current (horizontal lines) is well confined to the ISs. Fig. 1b presents the SC potentials (thick lines) together with the position dependent electrochemical potentials (thin lines). We observe that at the large bias the Hall potential tilts the LLs. Note that, since the compressible regions can almost perfectly screen the Hall potential, the major effect on the $\mu^*(x)$ is observed at the regions where an IS resides. Now, we investigate the effect of current bias induced density asymmetry at the asymmetrically depleted samples. In Fig.2 (black) solid curves present $\nu(x)$ of a generic sample. For the lowest B value (a), no ISs exist larger than λ (see the inset) for the symmetric and negatively biased asymmetric (dash-dotted blue curves) samples. Therefore, the electron and the current densities both remain symmetric (note that the system is completely compressible), hence the induced Hall potential can be almost perfectly screened. The current distribution exhibits, local spikes at the positions of $\nu(x) \approx 2$ since, $\rho_L(x)$ assumes very small values in the very close vicinity of $\nu(x) = 2$, although no IS exists. One can clearly see that some amount of current is still flowing from the bulk. However, for the asymmetric sample under (+) bias (broken red lines) the IS on the RHS is larger than λ , hence, the current is confined within this region mainly, meanwhile no current flows from the bulk. We observe that for this B value, the generic and asymmetric (-) samples are out of the QHP. When increasing B slightly (Fig. 2b), an IS is now well developed on the RHS of the generic sample where most of the current is confined to, however, due to the local minima at the LHS mention before some current also flows from this side. The interesting point is that now no current flows from the bulk (up to our numerical accuracy, i.e, 10^{-14} A) and the system is in a QHP both for generic and asymmetric (+). Increasing the B field furthermore, results in formation of an IS also at the asymmetric (-) sample, where all three samples are in the plateau regime. When the center ν becomes very close to two (not shown here) the two ISs merge at the bulk and all the current is now flowing from the *incompressible bulk*, slightly asymmetric with respect to the center. At the highest B field strengths shown in Fig.3, the system is out of the QHP and both the electron and the current densities become symmetric, again. If compared to Ahlswede experiments the sequence of the potential types is I-I-III-III-II-I, which perfectly matches with the findings. It is reasonable to expect that, if one

starts already with an asymmetric density profile, the asymmetry induced by the large current will be either enhanced or suppressed depending on the current direction. A (+) bias will tilt the LLs resulting a high potential on the RHS, whereas a (-) bias will do the opposite. Therefore, for the (+) bias the sequence is I-III-III-III-II-I, which essentially means that the asymmetric sample enters to the QHP at a lower B field compared to a generic sample, due to already existing large IS at the RHS. The situation is rather different for the (-) bias, since the narrow IS is on the LHS and the high bias will enlarge this IS. Hence, there is a competition between the slope of induced Hall potential and the confinement potential to generate a wide IS. Thus, the asymmetric sample when (-) biased will enter to the QHP at a higher B field value compared to both (+) biased and generic samples. The asymmetric distribution of the ISs is obvious for the generic sample, where we only show the ISs (dark-blue regions) wider than λ . Our findings point out that the extend of the QHPs depend strongly on the sample asymmetry and the current polarization. The experimental manifestation of the predicted rectification effect requires, first of all, high mobility ($\geq 1.0 \times 10^6$ cm²V/s) and narrow ($2d \lesssim 10$ μ m) asymmetrically depleted samples. One possible option is to define the Hall bars similar to the ones investigated in Ref. [13], at which, an asymmetry in R_L is observed. However, the effect is not pronounced to draw clear conclusions. The main drawback of the gate defined samples relies on the fact that, by using gates one cannot create very steep edge potential profiles, therefore, rectification is somewhat suppressed. Meanwhile, one can define Hall bars with steeper edge potentials by deep etching, of course, with different etching depth on both sides. However, it is known that etching can cause inhomogeneities at the density profile which may become important when considering narrow samples. A hybrid solution, i.e. one side etch, other side gate defined, seems to be the most reasonable solution. To obtain the extreme sharp edge on one side, it is desirable to perform the suggested experiments on cleaved edge overgrown (CEO) samples, where it has been shown that no ISs reside at the sharp edge [16]. The experiments need not to be done at very low temperatures ($0.4 < T < 4.0$ K), whereas the imposed current should not exceed the breakdown current due to Joule heating [9], which can easily be determined by the experiments.

In conclusion, for the high mobility, narrow and asymmetric samples we predict that, the large current either enlarges or shrinks the QHPs depending on whether the asymmetry induced by the current and the asymmetry caused by the edge profile coincides or not. Based on our findings, we proposed three set of sample structures where the effect of the current induced asymmetry and thereby the rectification of the QHPs can be controllably measured. As a final remark, we note that at the edge IQHE regime, i.e. Type III, a highly non-equilibrium

situation is present, due to the competition between the enhancement of the ISs resulting from the large current and suppression due to steep potential profile, therefore we expect a hysteresis like behavior in this regime both depending on the sweep rate and direction of the B field and current amplitude.

Author acknowledges M. Grayson for fruitful discussions concerning the CEO samples, R. R. Gerhardts for his valuable suggestions and K. Güven for his contribution to extend our work to the non-linear regime. This work was financially supported by NIM area A and DIP.

-
- [1] K. v. Klitzing, G. Dorda, and M. Pepper, *Phys. Rev. Lett.* **45**, 494 (1980).
 - [2] R. B. Laughlin, *Phys. Rev. B* **23**, 5632 (1981).
 - [3] B. I. Halperin, *Phys. Rev. B* **25**, 2185 (1982).
 - [4] M. Büttiker, *IBM J. Res. Dev.* **32**, 317 (1988).
 - [5] D. B. Chklovskii, B. I. Shklovskii, and L. I. Glazman, *Phys. Rev. B* **46**, 4026 (1992).
 - [6] A. M. Chang, *Solid State Commun.* **74**, 871 (1990).
 - [7] K. Güven and R. R. Gerhardts, *Phys. Rev. B* **67**, 115327 (2003).
 - [8] A. Siddiki and R. R. Gerhardts, *Phys. Rev. B* **70**, 195335 (2004).
 - [9] S. Kanamaru, H. Suzuura, and H. Akeru, *J. Phys. Soc. Jpn.* **75** (2006), and proceedings EP2DS-14, Prague 2001.
 - [10] E. Ahlswede, J. Weis, K. von Klitzing, and K. Eberl, *Physica E* **12**, 165 (2002).
 - [11] S. Ilani, J. Martin, E. Teitelbaum, J. H. Smet, D. Mahalu, V. Umansky, and A. Yacoby, *Nature* **427**, 328 (2004).
 - [12] K. Lier and R. R. Gerhardts, *Phys. Rev. B* **50**, 7757 (1994).
 - [13] J. Horas, A. Siddiki, J. Moser, W. Wegscheider, and S. Ludwig, *Physica E Low-Dimensional Systems and Nanostructures* **40**, 1130 (2008), arXiv:0707.1142.
 - [14] T. Ando, A. B. Fowler, and F. Stern, *Rev. Mod. Phys.* **54**, 437 (1982).
 - [15] D. B. Chklovskii, K. A. Matveev, and B. I. Shklovskii, *Phys. Rev. B* **47**, 12605 (1993).
 - [16] M. Huber, M. Grayson, M. Rother, W. Biberacher, W. Wegscheider, and G. Abstreiter, *Phys. Rev. Lett.* **94**, 016805 (2005).